I&EC research
Industrial & Engineering Chemistry Research

pubs.acs.org/IECR

Article

Synthesis of ZIF-8 Membranes on γ-Alumina Supports for Separation of Propylene/Propane Gas Mixture

Fateme Banihashemi and Jerry Y. S. Lin*

Cite This: *Ind. Eng. Chem. Res.* 2022, 61, 4125−4133

Read Online

ACCESS | Metrics & More | Article Recommendations

ABSTRACT: Zeolitic imidazolate framework-8 (ZIF-8) membranes have shown promising potential for the separation of industrially important propylene/propane mixtures. For industrial applications, it is necessary to synthesize a thin and defect-free ZIF-8 membrane with good integrity on scalable supports. In this work, we report the synthesis of ZIF-8 membranes on the sol−gel derived mesoporous γ-alumina layer coated on top of the α-alumina support. Thin (2.5 μm), high quality, and stable ZIF-8 membranes can be grown on the γ-alumina support grafted with 3-glycidoxypropyltrimethoxysilane (GLYMO) by the seeded secondary growth method. Propylene/propane equimolar mixture separation experiments were conducted to test the separation performance of membranes. Compared to the ZIF-8 membranes on the bare macroporous α-alumina support, ZIF-8 membranes prepared on the γ-alumina coated α-alumina support show much better separation characteristics, with a maximum propylene/propane separation factor of 225 and propylene permeance of 9.65 × 10^{-9} mol m^{-2} s^{-1} Pa^{-1}. The ZIF-8 membrane synthesized on the scalable γ-alumina coated α-alumina support exhibits separation characteristics and stability similar to the best-performing ZIF-8 membranes on alumina supports with complex synthesis procedures difficult to scale up.

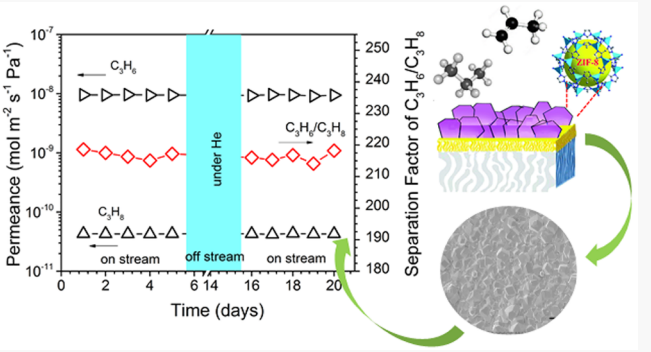

INTRODUCTION

The development of energy-efficient and sustainable approaches for propylene/propane separation is of paramount significance in petrochemical industries.[1,2] Considerable energy and capital cost savings are possible by applying membrane-based separation technology.[3,4] Membranes made of zeolitic imidazolate frameworks (ZIFs),[5,6] particularly ZIF-8,[7] offer great perspective for future usage in industrial propylene/propane separation. Toward this goal, it is important to develop efficient, scalable methods for reproducible synthesis of defect-free ZIF-8 membranes on practical porous supports.[8,9]

Significant progress has been made in depositing thin ZIF-8 layers on various types of inorganic[10−12] and porous ceramic[5,13] substrates by solution-based methods. Porous ceramic substrates provide structural integrity, have the advantage of high thermal, mechanical, and chemical stability, and thus are considered as ideal substrates for ZIF-8 membranes.[14,15] The most important surface characteristics of the ceramic substrate that could influence ZIF-8 film growth are pore size, surface roughness, and chemical composition. Of these three factors, the chemical composition of the support has the largest influence on crystal nucleation and growth.[16,17] ZIF-8 membranes are commonly synthesized on macroporous α-alumina substrates.[18−21] However, relatively low propylene permeances were reported when the α-alumina disk was used as a substrate.[7,22] Furthermore, the widely used α-Al_2O_3 supports have quite large pores (pore diameter > 150 nm), leading more likely to discontinuous and/or nonhomogeneous ZIF-8 film formation.[23]

ZIF-8 membranes were also grown on other inorganic supports. Isaeva and co-workers[24] synthesized ZIF-8 membranes via direct in situ crystallization on a composite aluminum zirconate-based support for He separation. They found that the nature of the support and texture (microporous and macroporous) affect the morphology of the ZIF-8 selective layers on the membrane surfaces. Caro and co-workers[25] reported fabrication of a 40 μm thick ZIF-8 layer on an asymmetric porous titania substrate by a direct growth method using microwave-assisted heating for hydrogen separation. However, expensive raw material for the synthesis of zirconium-based support, lack of stability of a titanium

Received: December 21, 2021
Revised: February 17, 2022
Accepted: February 25, 2022
Published: March 8, 2022

https://doi.org/10.1021/acs.iecr.1c04986
Ind. Eng. Chem. Res. 2022, 61, 4125−4133

substrate, and a complicated preparation process had limited their applications.[26] The preparation of the ZIF-8 membrane was documented by Dangwal et al.[7] on a silicalite-seeded anodic alumina oxide (AAO) substrate by the secondary growth method. They could fabricate high quality ZIF-8 membranes for propylene/propane separation due to the strong attachment of silicalite seed crystals to AAO substrates through hydrogen bonding. However, AAO substrates are brittle, fragile, and expensive, making it very difficult to scale up the synthesis of ZIF-8 membranes on the support.[27,28]

The sol−gel derived γ-alumina membranes are mesoporous and offer a smooth surface for growing microporous membranes.[29,30] Choi and co-workers[23] reported synthesis of ZIF-8 membranes on the γ-alumina coated α-Al_2O_3 disc by an in situ counter-diffusion method. The supports consist of hierarchically structured γ-Al_2O_3/α-Al_2O_3 layers. The γ-Al_2O_3 layer was used to control the counter-diffusion of the Zn source and 2-methylimidazole ligand, leading to formation of a ZIF-8 layer within the support with the γ-Al_2O_3 layer serving just as a protective layer for the ZIF-8 separation layer. Tsapatsis and co-workers[3] reported the fabrication of ZIF-8 nanocomposite membranes by means of atomic layer deposition (ALD) of ZnO in the porous alumina support. During ALD, diethylzinc reacts with the surface hydroxyl groups, followed by ligand-vapor treatment, in the mesopores of the γ-alumina layer. Their membranes showed a maximum separation factor of 152 and propylene permeance of 3.68×10^{-8} mol m^{-2} s^{-1} Pa^{-1} with the vacuum pressure on the permeate side using the time-lag technique. However, the ALD technique for synthesis of the ZIF-8 membrane is expensive and not easily scalable.[31,32] Nevertheless, these studies show promise with the use of α-alumina macroporous substrates coated with a γ-alumina mesoporous layer with pores in the 2−5 nm range for growing high quality ZIF-8 membranes.

The γ-alumina coated α-alumina supports can be readily prepared by the scalable sol−gel method,[33] and there are, in fact, ultrafiltration membranes commercially available from several companies. On the other hand, seeded secondary is also a scalable method for the synthesis of microporous membranes such as those of zeolite and metal−organic frameworks. The objective of this work is to explore the synthesis of high performance ZIF-8 membranes on the sol−gel derived γ-alumina layer using the simple and scalable seeded secondary growth method. The work compares the C_3H_6/C_3H_8 mixture separation performance of the ZIF-8 membranes on the γ-Al_2O_3/α-Al_2O_3 support with those of ZIF-8 membranes on the intact α-Al_2O_3 supports without γ-Al_2O_3 to show the effectiveness of choosing a mesoporous support with a smooth surface for the synthesis of high performance ZIF-8 membranes.

2. EXPERIMENTAL SECTION

2.1. Synthesis of the α-Alumina Support with the γ-Alumina Layer and Grafting Modification. Macroporous α-alumina disk supports (2 mm thick, 20 mm in diameter, with an average pore diameter of 200 nm and porosity of 45%) were synthesized using A-16 α-alumina powder (Almatis, USA) by the press and sintering method as described in our previous publication.[34] A mesoporous γ-alumina layer was coated on the α-alumina disks by the sol−gel method. A boehmite sol was prepared from hydrolysis and condensation of aluminum tributoxide as previously reported[30] and then dip-coated on the polished side of α-alumina disks. The boehmite coated α-alumina supports were subsequently calcined at 550 °C for 3 h with a heating and cooling rate of 0.58 °C/min. The coated boehmite was converted to the γ-alumina layer bound to the α-alumina support in this calcination step. The γ-alumina layer was finally modified by grafting 3-glycidoxypropyltrimethoxysilane (GLYMO). This was done by immersing α-alumina supported γ-alumina disks in a GLYMO/ethanol solution (1.9 g of GLYMO, 20 mL of ethanol) at 40 °C for 30 min. The disks were removed from the solution, dried in air, and finally heat-treated at 100 °C for 4 h.

2.2. Synthesis of the ZIF-8 Seed Layer. ZIF-8 crystals for membrane seeding were prepared by the method of Cravillon and co-workers.[35] Zinc nitrate hexahydrate (734.4 mg, $Zn(NO_3)_2{\cdot}6H_2O$, ≥98%, Sigma-Aldrich) and 810.6 mg of 2-methylimidazole (MeIM, >99.0%, Sigma-Aldrich) were dissolved separately in 50 mL of methanol (MeOH, ≥99.5%, Sigma-Aldrich) to obtain clear solutions. The zinc solution was added into the imidazole solution slowly and stirred for 30 min followed by aging for 24 h. The resultant white colloidal solution was centrifuged (10,000 rpm) for 15 min to collect the particles. The obtained seeds were washed repeatedly using pure methanol and then dried under vacuum at room temperature for 24 h. To form the seeding suspension, 0.04 g of dried ZIF-8 crystals was dispersed in a glass vial containing 100 mL of methanol, followed by sonication for 30 min. The ZIF-8 seed layer was coated on the γ-alumina substrate by dip-coating. A ZIF-8 seed suspension of 0.05 wt % was used. The surface of γ-alumina substrates was brought in contact with the ZIF-8 seeding suspension for 20 s. The seeded supports were then dried in ambient air at room temperature for 10 min. The dip-coating procedure was repeated two times to ensure good coverage of the seed layer. The seeded supports were heat-treated at 95 °C for 3 h (with a heating and cooling rate of 0.3 °C/min).

2.3. Synthesis of ZIF-8 Membranes. The ZIF-8 seed layer was grown to a continuous layer by placing the seeded support vertically in a Teflon holder immersed in the secondary growth solution containing 2.27 g of MeIM and 0.11 g of $Zn(NO_3)_2{\cdot}6H_2O$ in 40 mL of deionized water in a Teflon lined stainless steel autoclave under hydrothermal conditions at 130 °C for 7 h. The synthesized membranes were washed with methanol several times followed by immersion in methanol at room temperature for 12 h. The membrane was then removed from methanol and dried under ambient conditions for 24 h. The secondary growth step was repeated with the hydrothermal treatment at 130 °C for 6.5 h to ensure sealing the intercrystalline gaps.

2.4. Characterization. Membrane surface morphology was studied by SEM (Amray 1910 with an accelerating voltage of 10 kV after gold/palladium deposition). The crystallographic properties of the α-alumina supported ZIF-8 membranes were examined by XRD (Siemens D5000, with a scan step of 2°/min for 2θ, using Cu K_α radiation (λ = 0.1543 nm) at 30 kV and 30 mA). Water contact angle analysis of ZIF-8 membranes was conducted using a Kruss Easy Drop Contact Angle apparatus equipped with a CCD camera. A water droplet (4 μL) was dropped on the external surface of membranes at four different points. Measurements were conducted at ambient pressure in 21−23 °C. The contact angle was measured after each drop was settled for 1 min, with the help of Droplet Shape Analyzer software.

2.5. Gas Separation. In studying membrane separation performance, a ZIF-8 membrane was sealed with Viton O-rings

https://doi.org/10.1021/acs.iecr.1c04986
Ind. Eng. Chem. Res. 2022, 61, 4125−4133

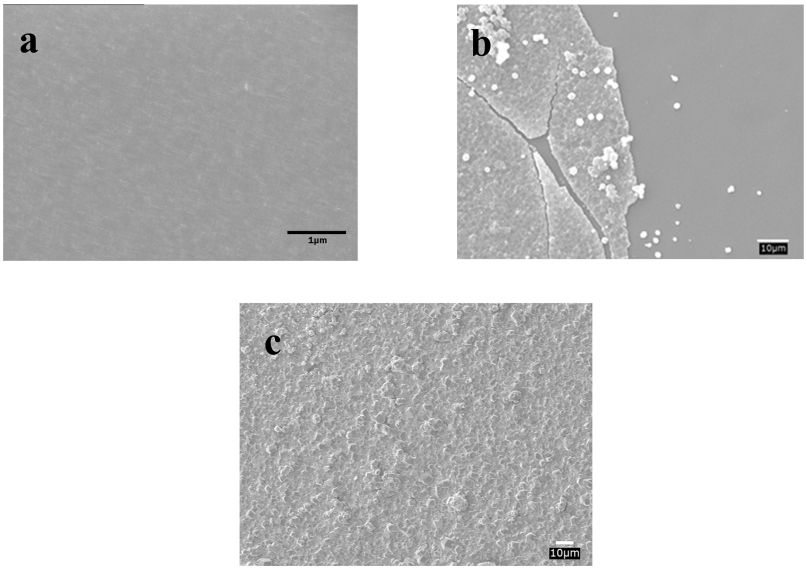

Figure 1. Surface SEM images of (a) the γ-alumina layer coated on the α-alumina support, (b) the ZIF-8 membrane synthesized on the α-alumina supported γ-alumina layer without modification, and (c) the ZIF-8 membrane on the α-alumina supported γ-alumina layer treated with GLYMO.

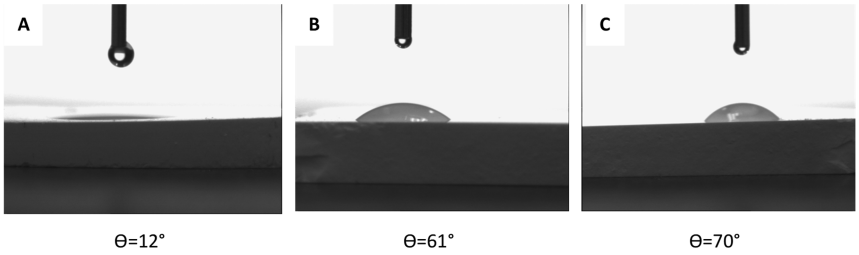

Figure 2. Static water surface contact angle micrographs of (A) the γ-alumina layer on the α-alumina support, (B) the γ-alumina layer after GLYMO treatment, and (C) the γ-alumina layer after treatment with H_2O_2 and then GLYMO.

(O-rings West, U.S.A.) in a custom-made stainless-steel permeation cell, and the effective permeation area was 2.27 cm^2. Binary gas separation experiments were conducted under the feed pressure of 1−2 atm using the Wicke-Kallenbach technique.[36] An equal molar propylene/propane mixture was fed to the membrane at a total feed flow rate of 100 mL/min using Brook's mass flow controllers. The membrane permeate side was swept with nitrogen (N_2) at a flow rate of 50 mL/min. The compositions of permeate and retentate were determined by an Agilent 6895 gas chromatograph equipped with a TCD detector using a silica gel packed column (dimensions: 1.8 mL, 3.2 mm O.D.). For each experimental run, 3 to 5 samples were analyzed to obtain the standard deviation of the permeance and separation factor. The accuracy of the gas permeation results was ±3.0%.

3. RESULTS AND DISCUSSION

3.1. Characteristics of Synthesized γ-Alumina Supports and ZIF-8 Membranes. Figure 1 shows the SEM images of the γ-alumina layer on the α-alumina support, the ZIF-8 membrane synthesized directly on the γ-alumina layer, and the ZIF-8 layer synthesized on the GLYMO treated γ-alumina layer. The SEM image of the γ-alumina layer shows a smooth mesoporous layer on top of the α-alumina support. Besides providing a smooth surface, the γ-alumina layer also acts as a barrier for avoiding ZIF-8 formation in the interior of the α-alumina support. A fracture, crack, and peeling off problem was observed for the ZIF-8 membranes synthesized on the γ-alumina layer without modification (Figure 1b). However, the ZIF-8 layer on top of the GLYMO treated γ-alumina layer is uniform without any defect (Figure 1c). This indicates that in the absence of the GLYMO treatment, the bonding between the ZIF-8 film and the substrate is weak.

Water contact angles and IR spectra were measured to understand how GLYMO treatment changes the surface properties of the γ-alumina layer that favors bonding of the ZIF-8 membrane and support. Figure 2 shows the static contact angles of water on the γ-alumina and GLYMO treated γ-alumina layer. Upon GLYMO treatment, a much larger contact angle is shown on the surface of the γ-alumina layer, indicating a reduction of hydrophilicity of the γ-alumina layer due to the hydrophobic nature of the GLYMO. The contact angle is even larger for the γ-alumina layer first treated with H_2O_2 and then GLYMO. It shows that H_2O_2 pretreatment is more effective for functionalization of γ-alumina by GLYMO, making the surface less hydrophilic.

Figure 3 shows the IR spectra of the γ-alumina layer without and with GLYMO treatment, before and after having been coated with ZIF-8 seeds. As shown in Figure 3, the absorption band at 1630 cm^{-1} and the broad absorption band at 3400−3600 cm^{-1} are respectively related to the bending vibration and stretching vibration of the H_2O and −OH groups on the surface of the γ-Al_2O_3. For the γ-alumina layer, the −OH peak appears at 1630 and 3420 cm^{-1}. Additionally, the IR spectra includes some wide peaks at 400−1000 cm^{-1} corresponding to Al−O stretching.[37] Two characteristic peaks at 581 and 734

https://doi.org/10.1021/acs.iecr.1c04986
Ind. Eng. Chem. Res. 2022, 61, 4125−4133

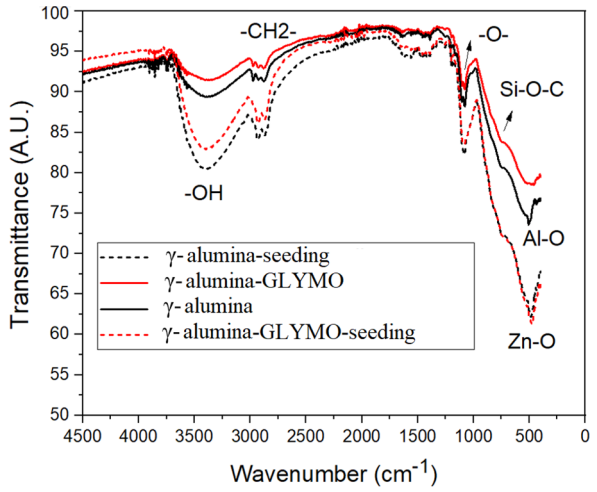

Figure 3. FT-IR spectra of γ-alumina before and after treatment with GLYMO and the seeding step.

cm^{-1} are assigned to the AlO_4 and AlO_6 stretching vibrations of Al−O bonding γ-Al_2O_3, respectively,[38] and the broad peak in this region indicates the presence of the γ-alumina phase.[39]

For GLYMO treated γ-alumina layers, the peaks at 2930 and 2840 cm^{-1} are related to asymmetric and symmetric stretching of the C−H band, respectively.[40] The absorption peaks at 2944, 2876, and 1470 cm^{-1} correspond to the CH_2 of GLYMO. In addition, the peaks at 1089 and 1194 cm^{-1} reveal the ether group (including the epoxy group), and the absorption peak at about 910 cm^{-1} corresponds to the Si−O−C bond of GLYMO.[41,42] Therefore, the characteristic peaks corresponding to CH_2 and OH appear in the same positions in Figure 3 for the γ-alumina and GLYMO.

ZIF-8 has four characteristic peaks at 2926, 1600, 1145, and 995 cm^{-1}, assigned to vibrations of C−H, C═N, and C−N in the imidazole ring, respectively. The sharp peak positioned at 457 cm^{-1} is attributed to the Zn−O stretching bonds.[43,44] This is the reason that this peak is more pronounced for the seeded samples in Figure 3.[7,45]

In this work, ZIF-8 membranes are synthesized on the γ-alumina layer in four steps, as schematically depicted in Figure 4. Based on the IR and water contact angle data, the mesoporous texture of the γ-alumina layer reduces defects in the α-alumina and provides a smooth surface for coating ZIF-8 seeds. However, the γ-alumina layer surface contains abundant surface hydroxyl groups and is highly hydrophilic. The ZIF-8 seed layer (and subsequently the ZIF-8 membrane) does not form a strong bond with the γ-alumina layer making the ZIF-8 coated layer prone to peeling off and formation of other defects. In the γ-alumina surface functionalization step, hydrolysis of three methoxyl groups of GLYMO molecules occurs initially. Then, the thermal treatment results in the condensation reaction of the hydrolyzed GLYMO with the hydroxyl groups of the γ-alumina layer. GLYMO molecules are attached to the γ-alumina layer via Si−O−Al bonds.[42,46] FTIR spectra also show reduction in OH-peak intensity of the samples after treatment due to binding the OH group with GLYMO molecules.

In the step of seeding, the ZIF-8 nanoparticles are grafted to the epoxy group of GLYMO via a ring-opening reaction.[7,42,45] Strong interfacial adhesion is constructed by chemical bonding between the ZIF-8 layer and the silane-modified γ-alumina layer. Once ZIF-8 nanoparticles contact the silane-modified substrate, the reaction between ZIF-8 and the GLYMO derived epoxy groups on the interface leads to the formation of Zn−O bonds resulting in good adhesion of the ZIF-8 coated seeds on the γ-alumina layer.[7,42] Finally, in the secondary growth step, the ZIF-8 seeds on the support surface grow into a continuous ZIF-8 film well bonded on the γ-alumina support.

Figure 5 shows SEM micrographs of the surface of the ZIF-8 seed layer (on γ-alumina) and the ZIF-8 membrane on the ZIF-8 seeded γ-alumina layer, the cross section of a ZIF-8 membrane synthesized on the γ-alumina coated α-alumina support in this work, and a representative ZIF-8 membrane on the α-alumina support. The ZIF-8 seed layer (Figure 5a) consists of ZIF-8 particles of uniform size less than 100 nm. Since a well-dispersed and stable seed suspension is used as the dip-coating sol, the aggregation of ZIF-8 particles is not observed. This continuous ZIF-8 seed layer provides

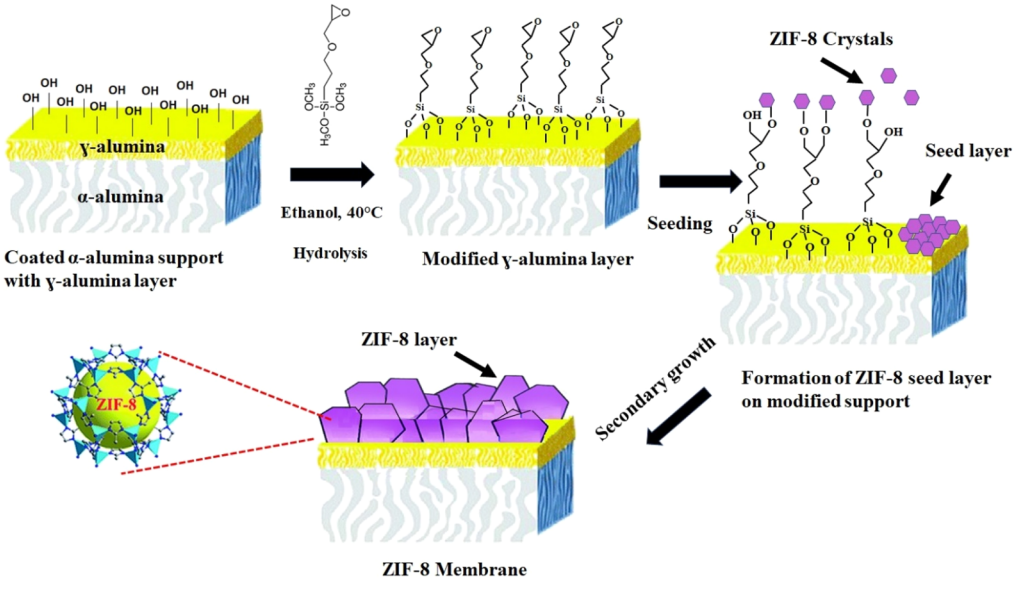

Figure 4. Suggested steps/mechanism for formation of the ZIF-8 membrane on the functionalized γ-alumina layer using GLYMO.

https://doi.org/10.1021/acs.iecr.1c04986
Ind. Eng. Chem. Res. 2022, 61, 4125−4133

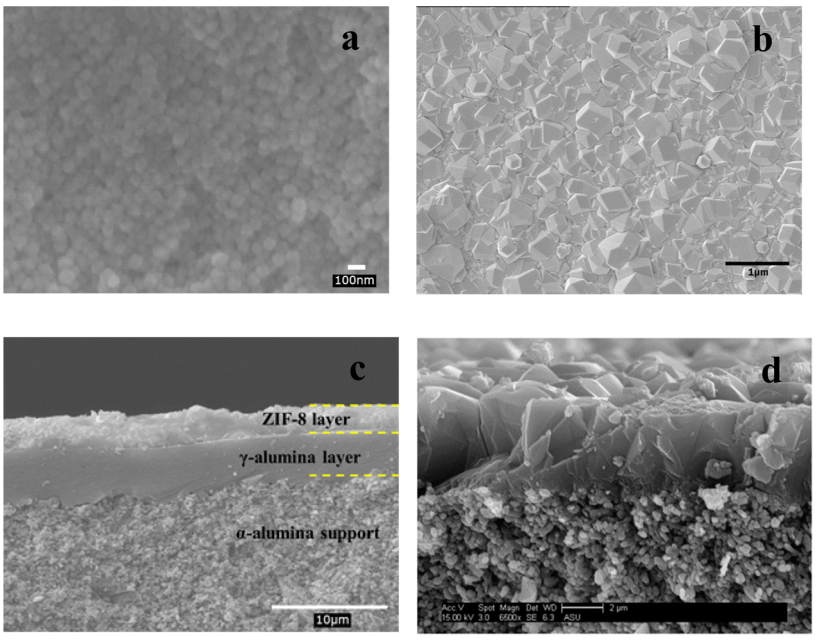

Figure 5. SEM micrograph top view of (a) the seeded γ-alumina layer, (b) ZIF-8 membrane, and (c) cross-section of the synthesized ZIF-8 membrane on the γ-alumina layer, and (d) cross-section of the ZIF-8 synthesized membrane on the α-alumina support (synthesized at 120 °C for 7 h).

nucleation sites for the secondary growth of ZIF-8 crystals into continuous film. The ZIF-8 membrane surface (Figure 5b) exhibits well-intergrown polycrystalline grains with high integrity without observable defects such as pinholes or cracks.

The cross-section micrograph of the ZIF-8 membrane (Figure 5c) clearly shows the ZIF-8 layer and the γ-alumina intermediate layer, respectively, of about 2.5 and 4 μm in thickness, and the α-alumina support. The ZIF-8 membranes on both γ-alumina (Figure 5c) and α-alumina (Figure 5d) are continuous, have a similar morphology, and do not have well-defined grain boundaries. However, the interface between the ZIF-8 membrane and γ-alumina is well-defined, and the thickness of the ZIF-8 layer on γ-alumina is about 2.5 μm. The ZIF-8 membrane on α-alumina (Figure 5d) does not show a clear boundary with the support suggesting some of the ZIF-8 crystals may penetrate in the support. The actual thickness of the ZIF-8 membrane on α-alumina could be higher than 2.5 μm suggested earlier[34] based on the continuous layer shown in the micrograph.

The XRD patterns of the α-alumina support, γ-alumina coated α-alumina substrate, and as-prepared ZIF-8 membrane are shown in Figure 6. The XRD pattern of the synthesized ZIF-8 membrane was obtained by XRD analysis of the surface of the dried membrane after the last secondary growth step. As shown, the XRD pattern of the ZIF-8 membrane is a combination of the diffraction patterns of the alumina support, γ-alumina intermediate layer, and ZIF-8 layer which is distinguished in Figure 6. The diffraction pattern of the ZIF-8 top layer agrees with the standard ZIF-8 crystal structure and confirms formation of random oriented polycrystalline ZIF-8 membranes.

3.2. Propylene/Propane Permeation and Separation Properties. Figure 7 shows the C_3H_6 and C_3H_8 permeances and C_3H_6/C_3H_8 separation factor for the ZIF-8 membrane synthesized on γ-alumina with increasing C_3H_6 concentration in the feed mixture. Similar results for the ZIF-8 membrane synthesized on the bare α-alumina[34] are also given for

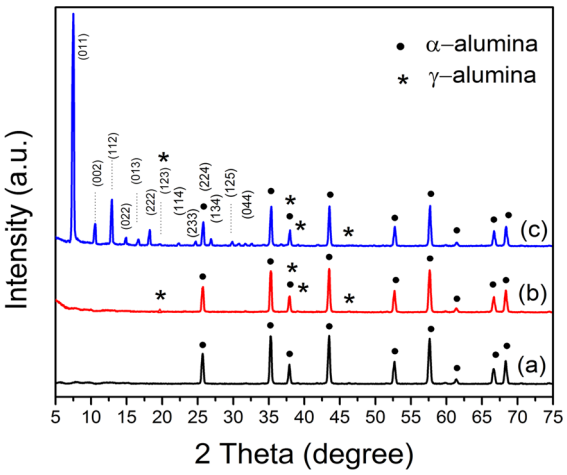

Figure 6. XRD patterns of (a) the α-alumina support, (b) γ-alumina layer on the α-alumina support, and (c) ZIF-8 membranes synthesized on the γ-alumina coated α-alumina.

comparison. As shown in Figure 7a and b, both ZIF-8 membranes have similar C_3H_6 permeance because these two membranes have similar thickness. However, the ZIF-8 membrane on γ-alumina has a C_3H_6/C_3H_8 separation factor (about 225) significantly larger than the ZIF-8 membrane on α-alumina (about 35), indicating a much better quality of ZIF-8 membranes grown on γ-alumina with a smooth surface. Figure 7a also shows an increasing C_3H_8 permeance and a decreasing C_3H_6 permeance (and hence decreasing C_3H_6/C_3H_8) with an increasing C_3H_6 partial pressure for both ZIF-8 membranes. However, the ZIF-8 membrane on γ-alumina exhibits highly stable permeance and a separation factor with respect to change in feed composition than the ZIF-8 membrane on α-alumina.

https://doi.org/10.1021/acs.iecr.1c04986
Ind. Eng. Chem. Res. 2022, 61, 4125−4133

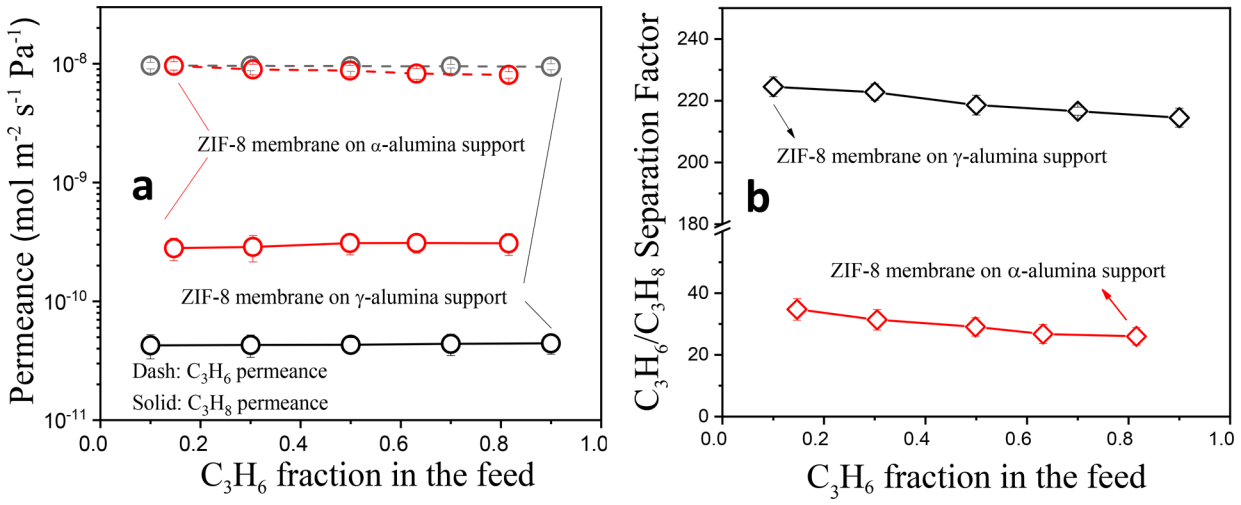

Figure 7. Effect of feed gas composition on the (a) C_3H_8 and C_3H_6 permeances and (b) C_3H_6/C_3H_8 mixture separation factor of ZIF-8 membranes synthesized on α-alumina and γ-alumina supports.

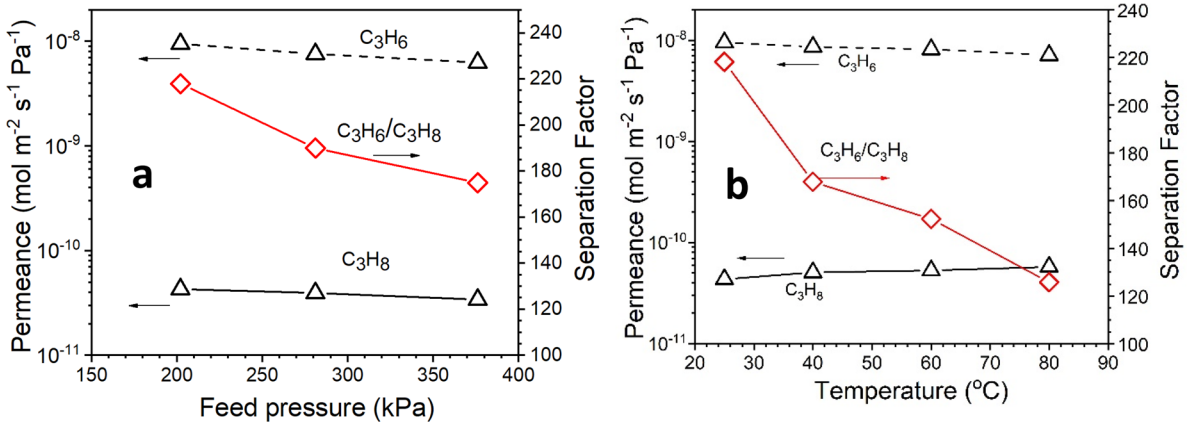

Figure 8. Feed pressure (a) and temperature (b) dependence of the permeance and separation factor of the C_3H_6/C_3H_8 binary mixture (50:50 feed) for a ZIF-8 membrane synthesized on γ-alumina. Temperature: 25 °C (a) and feed pressure: 205 kPa (b).

Gas permeance through a polycrystalline ZIF-8 membrane with intercrystalline gaps includes the contributions of flows through ZIF crystalline pores and intercrystalline gaps as[47]

$$F_i^{mea} = F_i^{ZIF} + F_i^{Int.} \quad (1)$$

The permeance through the intercrystalline gaps depends on intercrystalline pore size and porosity. Gas transports through the intercrystalline gaps can be assumed to follow the Knudsen mechanism. The measured separation factor is related to the membrane selectivity by

$$\alpha_{C_3H_6/C_3H_8} = \frac{F_{C_3H_6}^{mea}}{F_{C_3H_8}^{mea}} \quad (2)$$

combining eqs 1 and 2, and the observed separation factor is then determined by

$$\alpha_{C_3H_6/C_3H_8} = \frac{F_{C_3H_6}^{ZIF} + F_{C_3H_6}^{Int.}}{F_{C_3H_8}^{ZIF} + F_{C_3H_8}^{Int.}} \quad (3)$$

Data in Figure 7 show a 14% greater decrease in the C_3H_8 permeance followed by around a 25% greater decrease in the C_3H_6/C_3H_8 separation factor for the ZIF-8 membrane on α-alumina than the one on γ-alumina with the increasing C_3H_6 fraction in the feed side. This can be explained with the help of eqs 1−3 after further rearrangement. Since for C_3H_6 the permeation through ZIF-8 pores is much higher than the permeation through intercrystalline gaps ($F_{C_3H_6}^{ZIF} \gg F_{C_3H_6}^{Int.}$), eq 3 can be further simplified to

$$\alpha_{C_3H_6/C_3H_8} = \left[\frac{F_{C_3H_6}^{ZIF}}{F_{C_3H_8}^{ZIF}}\right]\left[\frac{1}{1 + \frac{F_{C_3H_8}^{Int.}}{F_{C_3H_8}^{ZIF}}}\right] \quad (4)$$

The measured separation factor decrease with increasing the C_3H_6 fraction in the feed side is magnified by the second term in eq 4, which is related to the existence of the intercrystalline gaps. For the ZIF-8 membrane on α-alumina, the C_3H_8 permeance through the intercrystalline gap is much higher than the one on γ-alumina. So, the good performance of as-prepared membranes on γ-alumina could be attributed to the highly intergrown ZIF-8 crystals in the ZIF-8 layer, and this limits the formation of nonselective permeation pathways through the layer.

Figure 8 shows the pressure and temperature dependency of the propylene/propane separation performance for the ZIF-8 membrane on the γ-alumina support. As shown in Figure 8(a),

https://doi.org/10.1021/acs.iecr.1c04986
Ind. Eng. Chem. Res. 2022, 61, 4125−4133

the permeances of both C_3H_6 and C_3H_8 decrease with increasing feed gas pressure at room temperature. Compared with that of C_3H_8, the permeance of C_3H_6 suffers a faster decline, and thus, the separation factor of C_3H_6/C_3H_8 drops with increasing feed pressure. These findings are consistent with the previous results of the effect of feed composition on separation performance. With respect to the temperature dependence (Figure 8b), the permeance of propylene decreases and that of propane increases with increasing temperature. It is known that the diffusion rate increases but adsorption (solubility) decreases with the increasing temperature. The increasing temperature may cause thermal expansion in pore size and may open up more defects which lead to a change of microstructure. This will decrease the molecular sieving effect and cause a reduction in the separation factor. ZIF-8 membranes on α-alumina have a similar temperature and pressure dependency of the C_3H_6 and C_3H_8 permeance.[34] The difference in selectivity and the permeance of propylene and propane is more determined by the difference in diffusivities of these gases in ZIF-8. Adsorption experiments showed that the two gases exhibit a similar sorption affinity in ZIF-8, but their diffusion rates differ by 2−4 orders of magnitude.[48] Propylene's slightly smaller kinetic diameter compared to propane allows it to pass more easily through the aperture of ZIF-8 crystals and diffuse much faster than propane. Thus, the aperture size of ZIF-8 crystals with respect to the molecular sizes of propylene and propane provides sharp molecular sieving for efficient separation of the propylene/propane mixture.[48,49]

Figure 9 shows permeation and separation performance of the C_3H_6/C_3H_8 mixture for a ZIF-8 membrane on γ-alumina

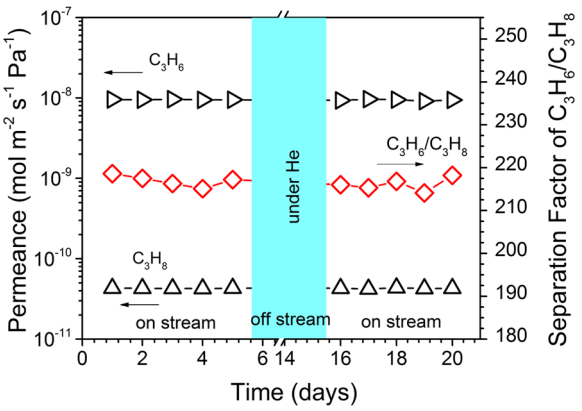

Figure 9. Separation results of C_3H_6/C_3H_8 mixture gases (50/50) on the ZIF-8 membrane as a function of time at 30 °C.

as a function of time, the first 5 days on the C_3H_6/C_3H_8 stream, then 10 days under He gas at room temperature, and then 5 days again on the C_3H_6/C_3H_8 stream. The ZIF-8 membrane exhibits good C_3H_6 permeance of about 10^{-8} mol/m^2·s·Pa (30 GPU) and the C_3H_6/C_3H_8 separation factor (about 220) during the entire period of tests. These results show good stability of the membranes on the γ-alumina support.

Figure 10 compares the C_3H_6/C_3H_8 separation performance of the ZIF-8 membranes on γ-alumina prepared in the present work with the separation performance for different ZIF-8 membranes on alumina supports published in the literature. Some publications on the ZIF-8 membrane synthesized on

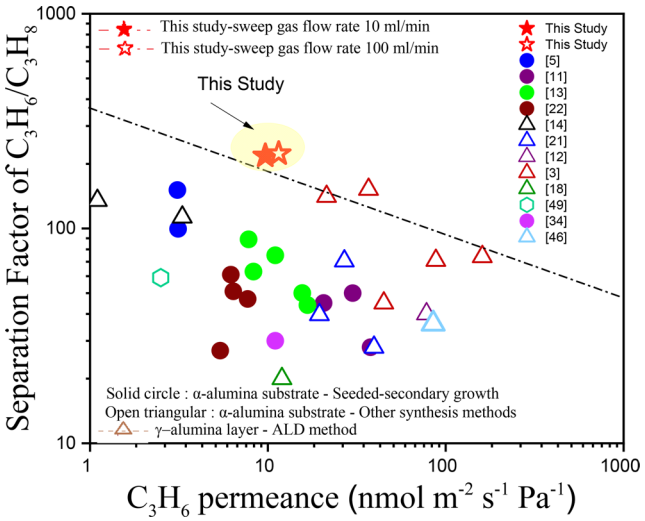

Figure 10. Comparison of the C_3H_6 separation performance of ZIF-8 membranes from the present work and literature.

polymeric and AAO substrates reported the C_3H_6/C_3H_8 separation factor and C_3H_6 permeance in the range of 10−300[6,50] and 0.1−6 × 10^{-8} mol m^{-2} s^{-1} pa^{-1},[10,51] respectively. However, the separation data from these membranes are not included in Figure 10 since the polymeric support cannot handle high temperature, and the AAO support is difficult to scale up for practical applications. As shown, the ZIF-8 membrane prepared in this work has the highest separation factor. ZIF-8 membranes prepared by Tsapatsis and co-workers[3] are comparable to the membrane reported in this work. Their membranes exhibit higher permeance and lower selectivity than those of the membranes synthesized in this study. This is due to the small thickness of their membranes (estimated thickness about 50 nm compared to the observed thickness of 2.5 μm of the membranes synthesized in this work), but their ZIF-8 membranes were prepared by atomic layer deposition (ALD) of ZnO in the porous γ-alumina support. The lower separation factor for the membranes prepared using the ALD method indicates the presence of some intercrystalline gaps in the membrane layer which could also lead to a higher permeance. The high performance of the ZIF-8 membranes synthesized in this work can be explained by the highly intergrown ZIF-8 crystals in the ZIF-8 film grown on the γ-alumina layer with minimized nonselective permeation paths through the layer.

4. CONCLUSIONS

Thin, high-quality ZIF-8 membranes can be grown on mesoporous γ-alumina coated α-alumina supports by the seeded secondary growth method. The γ-alumina layer needs to be functionalized by GLYMO to eliminate the γ-alumina surface hydroxyl groups leading to an enhanced bonding of the ZIF-8 layer with the support. The availability of the smooth mesoporous γ-alumina layer allows the synthesis of thin ZIF-8 membranes with well intergrown ZIF crystallites and minimum defects and intercrystalline gaps. The resulting ZIF-8 membranes exhibit superb propylene/propane permeation and separation characteristics. This work provides a simple and effective strategy to synthesize high performing ZIF-8 membranes on scalable and practical γ-alumina supports for industrial applications.

https://doi.org/10.1021/acs.iecr.1c04986
Ind. Eng. Chem. Res. 2022, 61, 4125−4133

AUTHOR INFORMATION

Corresponding Author

Jerry Y. S. Lin − *School for Engineering of Matter, Transport and Energy, Arizona State University, Tempe, Arizona 85287, United States;* orcid.org/0000-0001-5905-8336; Email: Jerry.Lin@asu.edu

Author

Fateme Banihashemi − *School for Engineering of Matter, Transport and Energy, Arizona State University, Tempe, Arizona 85287, United States*

Complete contact information is available at: https://pubs.acs.org/10.1021/acs.iecr.1c04986

Notes

The authors declare no competing financial interest.

ACKNOWLEDGMENTS

The authors gratefully acknowledge the financial support from the National Science Foundation of the United States (CBET-1511005, CBET-2031087). The authors thank Defei Liu for experiments on synthesis and characterization of ZIF-8 membranes on α-alumina supports.

REFERENCES

(1) Guo, M.; Kanezashi, M. Recent Progress in a Membrane-Based Technique for Propylene/Propane Separation. *Membranes* **2021**, *11* (5), 310.

(2) Lin, Y. S. Metal organic framework membranes for separation applications. *Current Opinion in Chemical Engineering* **2015**, *8*, 21−28.

(3) Ma, X.; Kumar, P.; Mittal, N.; Khlyustova, A.; Daoutidis, P.; Mkhoyan, K. A.; Tsapatsis, M. Zeolitic imidazolate framework membranes made by ligand-induced permselectivation. *Science.* **2018**, *361* (6406), 1008−1011.

(4) Lai, Z. Development of ZIF-8 membranes: opportunities and challenges for commercial applications. *Current Opinion in Chemical Engineering* **2018**, *20*, 78−85.

(5) Lang, L.; Banihashemi, F.; James, J. B.; Miao, J.; Lin, J. Y. S. Enhancing selectivity of ZIF-8 membranes by short-duration postsynthetic ligand-exchange modification. *J. Membr. Sci.* **2021**, *619*, 118743.

(6) Zhou, S.; Wei, Y.; Li, L.; Duan, Y.; Hou, Q.; Zhang, L.; Ding, L.-X.; Xue, J.; Wang, H.; Caro, J. Paralyzed membrane: Current-driven synthesis of a metal-organic framework with sharpened propene/propane separation. *Science advances* **2018**, *4* (10), No. eaau1393.

(7) Dangwal, S.; Ronte, A.; Lin, H.; Liu, R.; Zhu, J.; Lee, J. S.; Gappa-Fahlenkamp, H.; Kim, S.-J. ZIF-8 membranes supported on silicalite-seeded substrates for propylene/propane separation. *J. Membr. Sci.* **2021**, *626*, 119165.

(8) James, J. B.; Lang, L.; Meng, L.; Lin, J. Y. S. Postsynthetic Modification of ZIF-8 Membranes via Membrane Surface Ligand Exchange for Light Hydrocarbon Gas Separation Enhancement. *ACS Appl. Mater. Interfaces* **2020**, *12* (3), 3893−3902.

(9) Hou, Q.; Zhou, S.; Wei, Y.; Caro, J.; Wang, H. Balancing the Grain Boundary Structure and the Framework Flexibility through Bimetallic Metal-Organic Framework (MOF) Membranes for Gas Separation. *J. Am. Chem. Soc.* **2020**, *142* (21), 9582−9586.

(10) Wei, R.; Chi, H.-Y.; Li, X.; Lu, D.; Wan, Y.; Yang, C.-W.; Lai, Z. Aqueously Cathodic Deposition of ZIF-8 Membranes for Superior Propylene/Propane Separation. *Adv. Funct. Mater.* **2020**, *30* (7), 1907089.

(11) Pan, Y.; Li, T.; Lestari, G.; Lai, Z. Effective separation of propylene/propane binary mixtures by ZIF-8 membranes. *J. Membr. Sci.* **2012**, *390*−*391*, 93−98.

(12) Lee, M. J.; Kwon, H. T.; Jeong, H.-K. High-Flux Zeolitic Imidazolate Framework Membranes for Propylene/Propane Separation by Postsynthetic Linker Exchange. *Angew. Chem., Int. Ed.* **2018**, *57* (1), 156−161.

(13) Pan, Y.; Liu, W.; Zhao, Y.; Wang, C.; Lai, Z. Improved ZIF-8 membrane: Effect of activation procedure and determination of diffusivities of light hydrocarbons. *J. Membr. Sci.* **2015**, *493*, 88−96.

(14) Hara, N.; Yoshimune, M.; Negishi, H.; Haraya, K.; Hara, S.; Yamaguchi, T. Thickness Reduction of the Zeolitic Imidazolate Framework-8 Membrane by Controlling the Reaction Rate during the Membrane Preparation. *Journal Of Chemical Engineering Of Japan* **2014**, *47* (10), 770−776.

(15) Liu, L.; Luo, X.-B.; Ding, L.; Luo, S.-L. Application of Nanotechnology in the Removal of Heavy Metal From Water. In *Nanomaterials for the Removal of Pollutants and Resource Reutilization*; Elsevier: 2019; pp 83−147, DOI: 10.1016/B978-0-12-814837-2.00004-4.

(16) Zhou, M.; Nabavi, M. S.; Hedlund, J. Influence of support surface roughness on zeolite membrane quality. *Microporous Mesoporous Mater.* **2020**, *308*, 110546.

(17) Nair, S.; Tsapatsis, M. Synthesis and Properties of Zeolitic Membranes. In *Hand Book of Zeolite Science and Technology*; Auerbach, S. M., Carrado, K. A., Dutta, P. K., Eds.; Marcel Decker (New York): New York, 2003; Chapter 17, DOI: 10.1201/9780203911167.ch17.

(18) Hara, N.; Yoshimune, M.; Negishi, H.; Haraya, K.; Hara, S.; Yamaguchi, T. ZIF-8 membranes prepared at miscible and immiscible liquid-liquid interfaces. *Microporous Mesoporous Mater.* **2015**, *206*, 75−80.

(19) Kwon, H. T.; Jeong, H.-K.; Lee, A. S.; An, H. S.; Lee, J. S. Heteroepitaxially Grown Zeolitic Imidazolate Framework Membranes with Unprecedented Propylene/Propane Separation Performances. *J. Am. Chem. Soc.* **2015**, *137* (38), 12304−12311.

(20) Kwon, H. T.; Jeong, H. K. In situ synthesis of thin zeolitic-imidazolate framework ZIF-8 membranes exhibiting exceptionally high propylene/propane separation. *J. Am. Chem. Soc.* **2013**, *135* (29), 10763−8.

(21) Kwon, H. T.; Jeong, H.-K. Improving propylene/propane separation performance of Zeolitic-Imidazolate framework ZIF-8 Membranes. *Chem. Eng. Sci.* **2015**, *124*, 20−26.

(22) Yu, J.; Pan, Y.; Wang, C.; Lai, Z. ZIF-8 membranes with improved reproducibility fabricated from sputter-coated ZnO/alumina supports. *Chem. Eng. Sci.* **2016**, *141*, 119−124.

(23) Jang, E.; Kim, E.; Kim, H.; Lee, T.; Yeom, H.-J.; Kim, Y.-W.; Choi, J. Formation of ZIF-8 membranes inside porous supports for improving both their H_2/CO_2 separation performance and thermal/mechanical stability. *J. Membr. Sci.* **2017**, *540*, 430−439.

(24) Isaeva, V. I.; Barkova, M. I.; Kustov, L. M.; Syrtsova, D. A.; Efimova, E. A.; Teplyakov, V. V. In situ synthesis of novel ZIF-8 membranes on polymeric and inorganic supports. *Journal of Materials Chemistry A* **2015**, *3* (14), 7469−7476.

(25) Bux, H.; Liang, F.; Li, Y.; Cravillon, J.; Wiebcke, M.; Caro, J. Zeolitic Imidazolate Framework Membrane with Molecular Sieving Properties by Microwave-Assisted Solvothermal Synthesis. *J. Am. Chem. Soc.* **2009**, *131* (44), 16000−16001.

(26) Bashambu, L.; Singh, R.; Verma, J. Metal/metal oxide nanocomposite membranes for water purification. *Materials Today: Proceedings* **2021**, *44*, 538−545.

(27) Ying, Y.; Yang, Z.; Shi, D.; Peh, S. B.; Wang, Y.; Yu, X.; Yang, H.; Chai, K.; Zhao, D. Ultrathin covalent organic framework film as membrane gutter layer for high-permeance CO_2 capture. *J. Membr. Sci.* **2021**, *632*, 119384.

(28) Jeon, G.; Yang, S.; Byun, J.; Kim, J. Electrically Actuatable Smart Nanoporous Membrane for Pulsatile Drug Release. *Nano Lett.* **2011**, *11*, 1284−8.

(29) Ma, X.; Lin, B. K.; Wei, X.; Kniep, J.; Lin, Y. S. Gamma-Alumina Supported Carbon Molecular Sieve Membrane for Propylene/Propane Separation. *Ind. Eng. Chem. Res.* **2013**, *52* (11), 4297−4305.

(30) Cooper, C. A.; Lin, Y. S. Microstructural and gas separation properties of CVD modified mesoporous γ-alumina membranes. *J. Membr. Sci.* **2002**, *195* (1), 35−50.
(31) Patel, Y.; Janusas, G.; Palevicius, A.; Vilkauskas, A. Development of Nanoporous AAO Membrane for Nano Filtration Using the Acoustophoresis Method. *Sensors* **2020**, *20* (14), 3833.
(32) Oviroh, P. O.; Akbarzadeh, R.; Pan, D.; Coetzee, R. A. M.; Jen, T.-C. New development of atomic layer deposition: processes, methods and applications. *Sci. Technol. Adv. Mater.* **2019**, *20* (1), 465−496.
(33) Wang, Y.; Lin, Y. S. Sol-Gel Synthesis and Gas Adsorption Properties of CuCl Modified Mesoporous Alumina. *J. Sol-Gel Sci. Technol.* **1998**, *11* (2), 185−195.
(34) Liu, D.; Ma, X.; Xi, H.; Lin, Y. S. Gas transport properties and propylene/propane separation characteristics of ZIF-8 membranes. *J. Membr. Sci.* **2014**, *451*, 85−93.
(35) Cravillon, J.; Nayuk, R.; Springer, S.; Feldhoff, A.; Huber, K.; Wiebcke, M. J. C. o. M. Controlling Zeolitic Imidazolate Framework Nano- and Microcrystal Formation: Insight into Crystal Growth by Time-Resolved In Situ Static Light Scattering. *Chem. Mater.* **2011**, *23*, 2130−2141.
(36) Wicke, E.; Kallenbach, R. J. K.-Z. Die Oberflächendiffusion von Kohlendioxyd in aktiven Kohlen. *Kolloid-Z.* **1941**, *97*, 135−151.
(37) Jin, X.; Gao, L.; Sun, J.; Liu, Y.; Gui, L. Highly Transparent AlON Pressurelessly Sintered from Powder Synthesized by a Novel Carbothermal Nitridation Method. *American Ceramic Society* **2012**, *95* (9), 2801−2807.
(38) Wu, L.; Yin, Z. Sulfonic acid functionalized nano γ-Al2O3 catalyzed per-O-acetylated of carbohydrates. *Carbohydrate research* **2013**, *365*, 14−9.
(39) Park, Y. K.; Tadd, E. H.; Zubris, M.; Tannenbaum, R. Size-controlled synthesis of alumina nanoparticles from aluminum alkoxides. *Mater. Res. Bull.* **2005**, *40* (9), 1506−1512.
(40) Tabesh, S.; Davar, F.; Loghman-Estarki, M. R. Preparation of γ-Al_2O_3 nanoparticles using modified sol-gel method and its use for the adsorption of lead and cadmium ions. *J. Alloys Compd.* **2018**, *730*, 441−449.
(41) Bhowmik, K.; Pramanik, S.; Medda, S. K.; De, G. Covalently functionalized reduced graphene oxide by organically modified silica: a facile synthesis of electrically conducting black coatings on glass. *J. Mater. Chem.* **2012**, *22* (47), 24690−24697.
(42) Lou, Y.; Liu, G.; Liu, S.; Shen, J.; Jin, W. A facile way to prepare ceramic-supported graphene oxide composite membrane via silane-graft modification. *Appl. Surf. Sci.* **2014**, *307*, 631−637.
(43) Wu, C.; Liu, Q.; Chen, R.; Liu, J.; Zhang, H.; Li, R.; Takahashi, K.; Liu, P.; Wang, J. Fabrication of ZIF-8@SiO(2) Micro/Nano Hierarchical Superhydrophobic Surface on AZ31 Magnesium Alloy with Impressive Corrosion Resistance and Abrasion Resistance. *ACS Appl. Mater. Interfaces* **2017**, *9* (12), 11106−11115.
(44) Xiong, H.-M.; Shchukin, D. G.; Möhwald, H.; Xu, Y.; Xia, Y.-Y. Sonochemical Synthesis of Highly Luminescent Zinc Oxide Nanoparticles Doped with Magnesium(II). *Angew. Chem., Int. Ed.* **2009**, *48* (15), 2727−2731.
(45) Luanwuthi, S.; Krittayavathananon, A.; Srimuk, P.; Sawangphruk, M. In situ synthesis of permselective zeolitic imidazolate framework-8/graphene oxide composites: rotating disk electrode and Langmuir adsorption isotherm. *RSC Adv.* **2015**, *5* (58), 46617−46623.
(46) Tanaka, S.; Okubo, K.; Kida, K.; Sugita, M.; Takewaki, T. Grain size control of ZIF-8 membranes by seeding-free aqueous synthesis and their performances in propylene/propane separation. *J. Membr. Sci.* **2017**, *544*, 306−311.
(47) Banihashemi, F.; Meng, L.; Babaluo, A. A.; Lin, Y. S. Xylene Vapor Permeation in MFI Zeolite Membranes Made by Templated and Template-Free Secondary Growth of Randomly Oriented Seeds: Effects of Xylene Activity and Microstructure. *Ind. Eng. Chem. Res.* **2018**, *57* (47), 16059−16068.
(48) Zhang, C.; Lively, R. P.; Zhang, K.; Johnson, J. R.; Karvan, O.; Koros, W. J. Unexpected Molecular Sieving Properties of Zeolitic Imidazolate Framework-8. *J. Phys. Chem. Lett.* **2012**, *3* (16), 2130−2134.
(49) Krokidas, P.; Castier, M.; Moncho, S.; Brothers, E.; Economou, I. G. Molecular Simulation Studies of the Diffusion of Methane, Ethane, Propane, and Propylene in ZIF-8. *J. Phys. Chem. C* **2015**, *119* (48), 27028−27037.
(50) Brown, A. J.; Brunelli, N. A.; Eum, K.; Rashidi, F.; Johnson, J. R.; Koros, W. J.; Jones, C. W.; Nair, S. Interfacial microfluidic processing of metal-organic framework hollow fiber membranes. *Science* **2014**, *345* (6192), 72−75.
(51) Hara, N.; Yoshimune, M.; Negishi, H.; Haraya, K.; Hara, S.; Yamaguchi, T. Diffusive separation of propylene/propane with ZIF-8 membranes. *J. Membr. Sci.* **2014**, *450*, 215−223.

https://doi.org/10.1021/acs.iecr.1c04986
Ind. Eng. Chem. Res. 2022, 61, 4125−4133